NUMERICAL AND EXPERIMENTAL MODELING OF TITANIUM MESH CAGE DEVICE USED IN LUMBAR SPINE FUSION

Cleudmar Amaral de Araújo, cleudmar@mecanica.ufu.br
Fernando Lourenço de Souza, fernando.ldsmg@gmail.com
Gabriela Lima Menegaz, gabriela.menegaz@gmail.com
Valdico Faria, faria@mecanica.ufu.br
Federal University of Uberlândia, School of Mechanical Engineering – Av. João Naves de Ávila, 2121 – Campus Sta. Mônica, Uberlândia/MG-Brazil.

Irineu Vitor Leite, ileite@neoortho.com.br
Luciane Yumi Suzuki, lsuzuki@neoortho.com.br
Neoortho Orthopedics Products Corporation – Rua Ângelo Domingos Durigan, 607 – Cascatinha, Curitiba/PR-Brazil.

Abstrac: *Treatment of spinal deformities, degenerative diseases, injuries and tumors of the vertebral spine usually require the internal fixation system. In recent years, degenerative spinal instability has been effectively treated with cage. Stability failure of the vertebral fixation system may be correlated to the mechanical failures or to the failure in the interface between the bone tissue and the cage. However, little attention is focused on their design. The purpose of this study was to analyse the biomechanical behavior of a specific mesh cage in respect to the fatigue resistance and stress distribution when submited to a pure compression. This study employed a compression testing to determine cage resistance limits and fatigue testing to design for infinity life. A simplified finite element model was developed for available stress gradient in comparison to the fatigue testing results. Finally, a new 3D finite element model was developed using the mesh cage fixed between L3 and L5 vertebrae for obtaining the critical and failure regions. Analysis of the finite element models showed large stress concentration in the second, third and fourth cilindrical row of holes, according to the fatigue analysis. With pure compression, the cage analized can suport more than the charge applied in vivo.*

Keywords*: Cage, Lumbar Spine, Finite Element Model, Fatigue testing, Compression testing, Spinal implant.*

1. INTRODUCTION

A spine is formed by 33 vertebrae groups in 7 cervical, 12 dorsal, 5 lumbar at abdomen region, 5 fusion at sacrum level and 4 at lower forming the coccyx.

The effective decompression of spinal channel without occurrence of deformities and instability associated with nursing care simplified are basically included in treatment of spine pathology (MATUOKA e BASILE JÚNIOR, 2002).

Vertebral fixation systems are formed by anchorage components, stems and plates, accessories and transverse connectors. Neutralization loading is applied through the anchorage formed by components (BRANTLEY; MAYFIELD e KOENEMAN, 1994; BROWER et al., 1998; HIRANO; HASEGAWA e TAKAHASHI, 1997; KUHN et al., 1995; CHEN, LIN e CHANG, 2003).

Several lumbar spine diseases and traumas have been treated using fastening systems, like plates and screws, (YUAN et al., 1995). Although such systems provide good spine stabilization, some complications have been reported in the literature, such as pseudo-arthrodesis (GHANAYEM et. al., 1997). Cylindrical titanium cages have been used frequently in order to provide high level lumbar fusion resistance (BELLABARBA et. al., 2007).

The main advantage of titanium cages its biocompatibility that has the advantage of reducing infections and other complications (TENCER et. al. (1995)).

Geometrical cage characteristics, like holes along its body provide good flexibility, and allow better osseointegration, but decrease the axial loads and fatigue resistance. In this case, there are few studies of the mechanical behavior of spinal implants, mainly due to the difficulties in modeling.

Nandan et al.(2010) published an extensive literature review of the loading involving the intervertebral disks and the elements associated with spine interactions.

According to Panjabi et. Al. (1996) there are three types of biomechanical studies for the spine; Loading testing done through progressive load case up structural failure. Stability testing that evaluates the movement occurring at fixation systems under different sense applied loading. Finally, the fatigue testing that is done by cycle loading lower yield limit just to structural failure. In this case, the loading cycle is applied under maximum percentage compression load system normalized for ASTM F1704 and ASTM F1798 2003 (Standard Test Methods for Spinal Implants Constructs in a Vertebral Model).

Hirokawa et. al, (1998), evaluated the finite element method and concluded that the method allows a better understanding about the stress distribution applied for biomechanical engineering.

Currently, the finite element method (FEM) is used to design and evaluate possible in vivo failure. Simulation software based on this method allows the interaction analysis between the devices and bone rehabilitation, comparing

different prostheses, without needing to be tested in cadavers, requiring only a prior knowledge of the load conditions involved.

The purpose of this work is to evaluate the biomechanical behavior of a titanium mesh cage device applied to the lumbar spine and its resistance to fatigue and stress distribution when subjected to *in vivo* efforts. In parallel, two element finite models were developed for evaluating the critical regions subject to failure associated with gradient stress and comparing the results of fatigue testing.

2. MATERIALS AND METHODS

2.1. Spine biomechanics

The spine is a complex series of vertebral joints, has innate stability, promotes neural elements protection, rigid support, flexibility and segmental motion. It consists of 33 vertebrae; of which 24 are mobile contributing to the trunk movement. Vertebrae work in four curvatures that give balance and strength to the spine (HAMILL, KNUTZEN, 1999). The junction where one ends and the next curvature begins, is a place of greater flexibility and more vulnerable to injury (BERNHARDT M, BRIDWELL K H, 1989).

The vertebral body is cylindrical and thicker at the front. Between two vertebrae there is an intervertebral disk, which keeps the movement for shocks absorbable. Disks are capable of supporting compression, torsion and shear loading applied on the spine.

A disk hole is to support and to distribute the loads in the spine, as well as restricting the excessive movement that occurs in the vertebral segment.

A healthy intervertebral disk works hydrostatically and responds with flexibility in response to low loads and stiffness when it is subject to high loads. When the disk is overloaded in compression, the pulpous nucleus distributes the pressure on the disk uniformly and it acts as a shock absorber. It is very durable and seldom fails under compression. The cancellous bone of the vertebral body fractures before the damage occurs to the disk.

The critical region in the spine is formed by the lumbar vertebrae. Loads applied to the spine are produced by body weight, muscle strength acting on each mobile segment, pre-loads that are present due to the forces of the ligaments and the external loads that are being handled or applied.

Higher compression loading is sustained by the disk and vertebral body. The vertebral body is susceptible to injury before the disk, as shown in Figure 1.a, and it will fail with compressive loads, around 3700N for the elderly and 13000N for the young adult.

(a) (b)

Figure 1. (a) Fracture of disks under compression loading and (b) Disks Degeneration.

Spine lesion incidence is very high, and generally 60 to 80% of the population suffers from back pain at some point in life. According to Global Data® strategy studies, the global market for spinal implants is forecast to grow from $6.5 billion in 2009 to about $10.3 billion by 2016, with a Compound Annual Growth Rate (CAGR) of 7%. The global spinal fusion implants market is expected to reach a size of $9 billion by 2016. Market size in 2009 was $5.9 billion and is expected to grow annually at 6%. The spinal fusion implants segment is the biggest in terms of market size, contributing about 90% of the revenue for the spinal implants market category.

2.2. Titanium mesh cage

Since 1934 cages have been applied for spine arthrodesis. The first cylindrical mesh cage was implanted in 1986. Titanium cages proved to be most effective in follow-ups, no crashes or extrusions (HAO et. al., 2005). According to Ray (1997), this cage category was enough to have good bone fixation in 93% of the patients. Figure 2 shows an application case at cervical vertebrae fixation.

Figure 2. Titanium mesh cage implanted in cervical spine. Source: Chuang et. al (2006).

In most cases the surgical technique employing cages used expensive imported material. This study evaluated the biomechanical behavior of a titanium mesh cage made by Neoortho Orthopedics Products Corporation, Curitiba/PR, Brazil. The Cage evaluated was made of pure titanium, with 25 x 80 mm dimensions, holes of 5mm diameter, and 1.5mm thickness, shown in Figure 3.

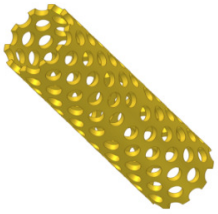

Figure 3. Titanium mesh cage made by Neoortho Orthopedics Products Corporation.

2.3. Fatigue testing on mesh cages

Cage yield strength can be obtained through a conventional compression testing determined by the maximum load reached during the testing, after the material's rupture. However, it is known that when dynamic forces are applied on the cage, it can break up with a load below the resistance limit, because of the material fatigue effect.

Material fatigue is the main reason of mesh cage failure, because the dynamic load effect present on the spine. Under repeated overload conditions associated with an inappropriate design, the implant can fail in a short time.

Some factors can accelerate the fatigue process, such as surface condition, stress concentration factor, environment conditions, and others. The cage break steps or any metallic material under fatigue are: crack nucleation, crack propagation until the material breaks.

In this work, basically the standard ASTM F2077-03 was used (Test Methods for Intervertebral Body Fusion Devices) and other details define 5 million of cycles for infinite life. Table 1 shows the standards used in experimental fatigue testing of the mesh cage. These conditions can be achieved, if the load is within the fatigue strength limit. Therefore, knowledge of these limits and the mechanical behavior of the cage, such as stress gradient are very important to obtain a good durability, since, in general, spinal surgery is painful, complex, risky and costly.

Table 1. Standards used for experimental testing.

Standard	**Description**
ASTM-F2077-03	Test Methods For Intervertebral Body Fusion Devices
ASTM-E1150	Definitions of Terms Relating to Fatigue
ASTM-E4	Standard Practices for Force Verification of Testing Machines
ASTM F67:06	Standard Specification for Unalloyed Titanium for Surgical Implant Applications
ASTM-E739	Standard Practice for Statistical Analysis of Linear or Linearized Stress-Life (S-N) and Strain-Life (ε-N) Fatigue Data

According to the standard ASTM-F2077-03, cage fail are related to permanent strain resulting from fracture or plastic strain. The fatigue strength limit of the implant is defined by load cycle number support before failure, Standard ASTM-E1150. Experimental testing was made in according to ASTM-E4. The specimen was made in according to ASTM F67:06, and the geometry by the standard ASTM-E739. The determination of the fatigue curve was made using a universal testing machine MTS-810, under cell load of 25KN.

The frequency cycle was fixed in 5Hz. According to standard ASTM-F2077-03, the load used was 75, 50 and 25% of the yield strength limit determined in advance by compression testing. The stopping criterion testing was 5 million of cycle, considered infinity life or cycle under local failure.

For preliminary testing, 5 specimens were used in compression and 6 specimens in fatigue testing, Figure 4. Table 3 show loading used at fatigue testing being F_{max} and F_{min} maximum and minimum loading, respectively. Percentage between yield loading and mean loading is represented for P% in table 3.

Figure 4. Mesh cages used in fatigue testing.

Table 3. Loading limits according to standard ASTM-F2077-03.

Specimens	F_{max} (N)	F_{min} (N)	$P_{\%}$
CP01	-14788	-1479	75.5
CP02	-14788	-1479	75.5
CP03	-10850	-1085	55.4
CP04	-10850	-1085	55.4
CP05	-7890	-789	40.3
CP06	-8880	-888	45.4

The fatigue criterion considered was the difference between the cyclic fatigue loading that results in "infinity life" and the cyclic fatigue loading that results in component failure should be less than 10% of the yield strength.

MPT software (Multi Purpose Testware) was used to obtain the displacements, loads and cycles number using MTS equipment. Figure 5 shows a mesh cage fixed to clamping jaws of MTS equipment.

Figure 5 – Mesh cage fixed to MTS clamping jaws.

2.4. Finite element models

The mesh cage should be implanted in the spine using auxiliary support plates for help at vertebral arthrodesis. In general, the Cage design allows good flexibility and mechanical strength and easy adaptation between vertebrae because its configuration through appropriated size at the moment of surgery. However the holes are points of stress concentration and modify the gradient stress along its length depending on loading applied.

knowledge about stress distribution is important despite the cage complex geometry mainly under compression loading since that load is more frequently applied into vertebrae. Critical points of the mesh cage can be shown through stress gradient indicating possible local failure of the cage through crack nucleation. These and other situations can be noted using finite element models.

The first finite element model was developed using the CAD geometry of the mesh cage being fixed into a cylindrical base metal-like assembly defined in fatigue testing. Geometry in SAT extension was exported to ANSYS® program and in a sequence a metal base was adding to fix the mesh cage. A finite element model was generated using solid 187 elements formed by 10 nodes and 3 degree of freedom by node, figure 6. Compression loading of 12800 N was applied at one end that corresponded at 64% of the material strength limit. At the other end the cylindrical base metal was fixed in all degree of freedom. Mechanical properties used in the model were, respectively, for steel mounted at metal base (Young modulus of 210 Gpa and Poisson coefficient of 0.30) and titanium mounted at mesh cage (Young modulus of 105 Gpa and Poisson coefficient of 0.34). Reference for yield limit used in mesh cage design was 500 Mpa.

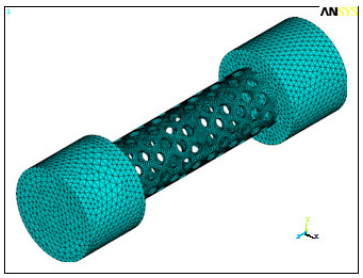

Figure 6. First finite element model of mesh cage tested.

A second finite element model was developed to understand the mechanical behavior of the mesh cage mounted between lumbar vertebrae and compression loading. In this case, it is possible to note the influence of vertebrae geometry configuration and boundary conditions in a mesh cage under load. Figure 7 shows the 3D finite element model developed and the geometric models used as reference to obtain the element mesh. The mesh cage was fixed between L3 and L5 lumbar vertebrae of an adult human. Here, the model studied simulated a replacement of L4 vertebra with a mesh cage. Vertebrae models were imported through tomography and manipulated in Solidworks program. SAT extension was export to Workbench Program which used 187 solid elements. To the upper vertebra a compression loading of 450 N was applied that simulates the trunk and limbs weight of a person of seventy kilos. The mesh cage was fixed in both vertebrae (L3-L5). Lower vertebra was fixed and loading was applied in line with geometry of upper vertebral body.

Mechanical proprieties of cortical bones was used in vertebrae models (Young`s modulus of 13.5 Gpa and Poisson coefficient of 0.3) and the same mechanical proprieties for titanium material used in mesh cage. All materials were considered homogeneous and isotropic for stress gradient analysis. Figure 7 shows the finite element model generated in the Workbench program for analysis of mechanical behavior.

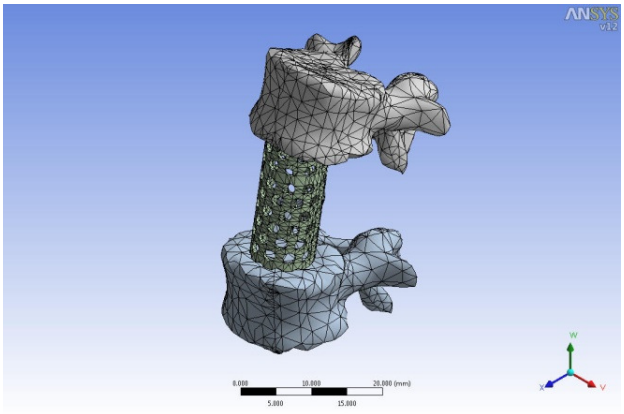

Figure 7. 3D Finite element model generated at Workbench Program.

3. RESULTS

Figure 8 shows results of loading versus displacement obtained by compression testing and Figure 9 shows two specimens after the compression testing.

It can be observed that plastic strain occurs next to the upper cage and its being higher in one side of the cage due to the possibility of upper inclination support. Table 4 shows the results obtained by the compression testing for all specimens analyzed. Where F_y and F_{ut} represent loading at yield and resistance limits, respectively. L_y and L_{ut} represent displacements at yield and resistance limits, respectively. Value of R_c indicates an equivalent stiffness of mesh cage.

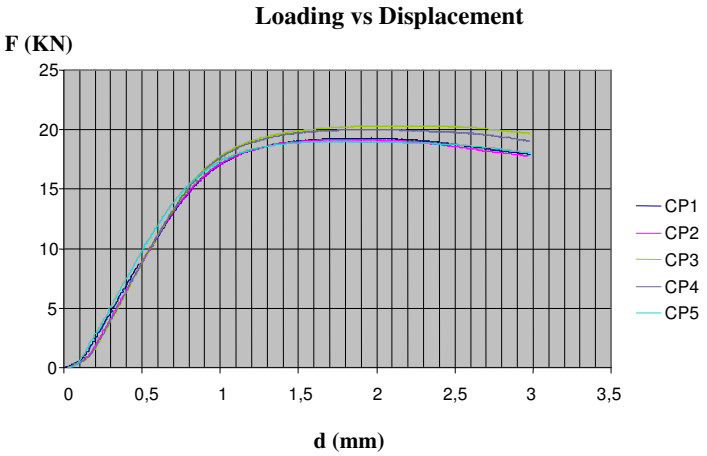

Figure 8. Loading versus displacement for specimens under compression testing.

Figure 9. End configuration of two specimens after compression testing.

Table 4. Results of compression testing.

Specimen	F_{ut} (N)	F_y (N)	L_{ut} (mm)	L_y (mm)	R_c (N/mm)
CP01	19191.1	12980	1.77	0.68	23770.9
CP02	19301.9	13900	1.97	0.73	23320.5
CP03	20347.6	13936	2.23	0.69	21562.1
CP04	20031.9	13890	2	0.68	21480
CP05	19031.6	13486	1.79	0.66	18377.5
Mean	19580.8	13638.4	1.95	0.69	21702.2
Standard deviation	575.1	411.4	0.2	0.01	2122.6

The testing sensibility to stop was 0,04 mm at maximum displacement. The value, where the micro crack in the specimen structure started, indicates the potential fail situation. The Figure 10 shows the semi-log curve for the experimental points obtained by fatigue testing, as well as the regression curve using the point (1000 cycles; 0.95 Fut) that is normally used to estimate the fatigue curve.

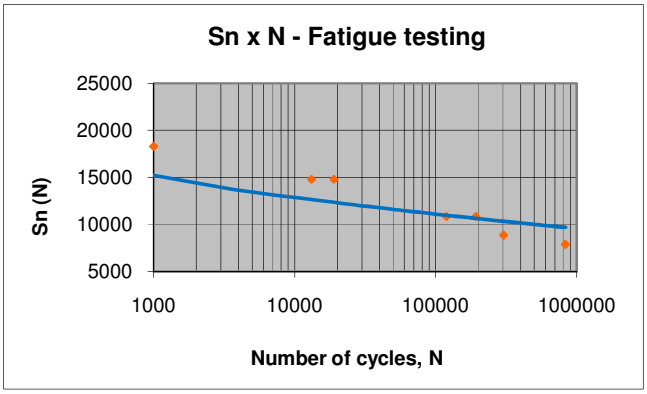

Figure 10. Fatigue resistance versus cycles number in semi-log scale.

Fatigue resistance prediction can be obtained by Equation 1 and 2, and the regression curve. So,

$$logS_n = loga + b * logN_c = -0.157logN_c + 4.832 \quad (1)$$

Therefore, b = -0.157 and a = 67920. So, the predictive equation for the fatigue resistance will be,

$$S_n = 67920{N_c}^{-0.157} \quad (2)$$

Using Equation 2 it is possible to estimate loading for infinity life (5 million of cycles) as being,

$$\mathrm{S_n} = 6029[\mathrm{N}] = 614[\mathrm{Kgf}] \quad (3)$$

The infinite life loading represents about 31% of the maximum load applied (Fut), as well as presented in the Table 4. Figure 11 shows equivalent stresses calculated on the first finite element model. It is possible to note that higher stress are located along the cage length at boundary holes mainly near the second and third row because of tridimensional and complex form of the model and loading case. Maximum values of stresses were 480 Mpa near the yield stress but located in small areas of holes. Regions located at central points and near the clamp show small stress values.

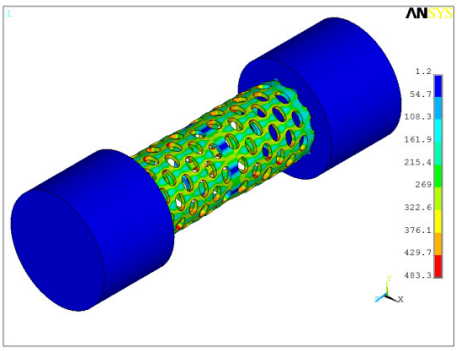

Figure 11. Equivalent stress at finite element models of mesh cage.

In the mesh cage tested we can see 12 rows with 11 holes of 5 mm diameter in each one. Two rows in central region are coincident such that a little big space is formed as compared to distance for the other row. Therefore, stress distribution is modified and it is possible to note in figure 11 that holes change the stress pattern along the length of the cage. Stress values of 10 Mpa will increase to middle to end. Those diminished stress return near the end of the cage. So, that row near the hole is able to cause cracks due to fatigue process. This effect was noted on fatigue testing as show in figure 12. Many tests showed initial failure about crack spreading from third upper row of hole.

Figures 13 and 14, show equivalent stress and total deformation for the second finite element model, respectively. Maximum values of stress were 380 Mpa at the second row of holes in the lower model. Because the boundary

conditions and simplifications of the model, since the ligaments and muscles were not considered and the bone graft was despised, the stress distribution is similar to the bending case of the mesh cage. Sharp edges of holes promotes higher stress and this fact can be observed at stress distribution and a new format could be machined with a rounding at local area. Displacements of 0.3 mm can be noted in upper areas of cage but again the values were higher because the boundary conditions and simplifications.

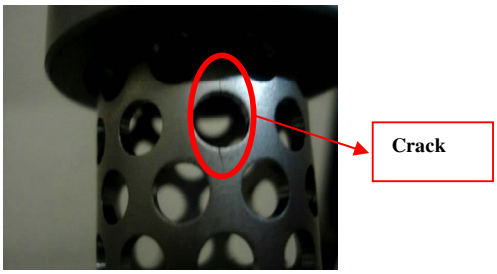

Figure 12. Crack noted at third row of holes on mesh cage during fatigue testing.

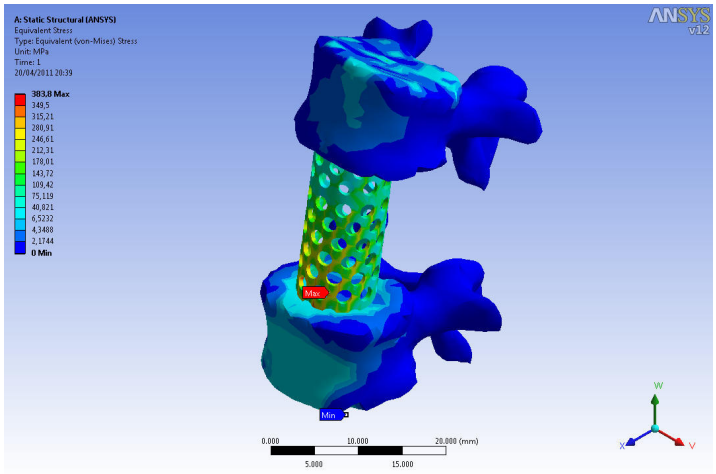

Figure 13. Equivalent stress of second finite element model using a mesh cage fixed between vertebrae.

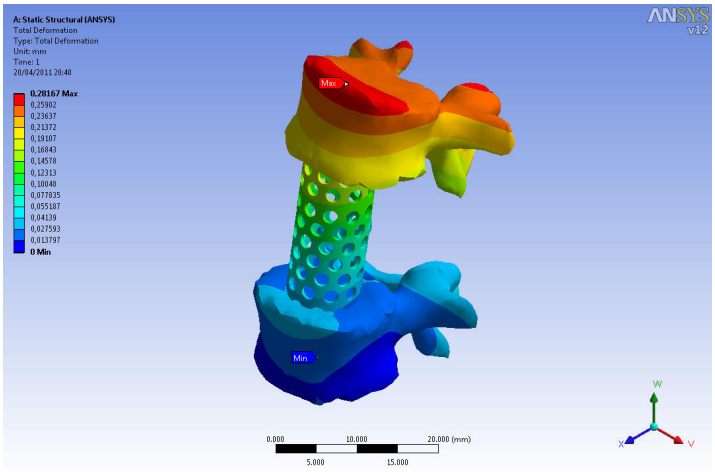

Figure 14. Total deformation at second finite element model showing displacements of cage.

4. DISCUSSION

Spine injuries require mostly internal fixation (Vaccaro et al., 1995; Matuoka e Basile Júnior, 2002). Failure in the stability of vertebral fixation system can be related to mechanical failure of implant or bone interface (Lastra e Benzel, 2003).

In recent years several cage system were developed for spinal arthrodesis treatment. Design of mesh cages seeing dynamic methods to obtain the fatigue resistance with finite element methods was not noted in literature though at this time a simplified model configuration was used.

Although there are several cage configurations, including bioresorbable materials, geometrically optimized models to take into consideration different loading into spine and its nonlinearities are not yet known.

Clinical research shows that the higher local stability improves the arthrodesis process and bone setting. Advantage of biomechanical testing for design of cages is related with real tests regardless of limitations about the boundary conditions adopted.

Through compression testing 1390 Kgf and 1994 Kgf for mean yield load and mean resistance load, respectively was obtained. Range of mean stiffness of cage was 22 KN/mm.

Holes present on mesh cage are stress concentration points and therefore failure or cracks tend to occur as noted in fatigue testing. In most specimens there were no changes in nominal size and cracks were not detected using non-destructive testing in sequence. For terminating test procedure used in fatigue testing was performed considering a variation of 0,04 mm in amplitude of the signals of displacement. Results of fatigue testing shows a load limit for infinite life of 614 kgf for mesh cage 25 mm diameter.

Finite element models were used for calculating the equivalent stress and total deformation of critical regions. Second and third rows of holes were the critical regions where initial failure was noted.

Length of mesh cage composed by rows is necessary to permit surgical insertion of the cage depending on patient biological characteristics. However it was observed in finite element analysis and fatigue tests that holes are stress concentration points and therefore are more critical. Possible design solutions would be to use a model with holes of different diameters by optimizing the cage geometry considering stress gradient lower and also to study the possibility of rounding edges of holes in such regions.

The goal of this study is to show an alternative methodology for assessing the mesh cage design to better understand its biomechanical behavior and providing such a methodology for other cage types.

This system was not tested in vivo, but the results of this study “in vitro” confirm its importance before a clinical application in order to detect critical regions and failures, increasing its useful life and promoting security and patient comfort.

Upgrading the cage designs for performing the spinal fusion is still necessary due to the complexity of spine loading and movements. Mesh cages can be used advantageously for fixation of vertebrae and replacement, as shown in the finite element model study. In general, these devices are inserted with screws and fixing plates and have advantages as additional element repairers to carry out the column stability. Therefore, future improvement of these devices will allow the inclusion of alternative systems of spinal fixation.

5. CONCLUSION

Design of mesh cages was analyzed using finite element models and fatigue testing. The mechanical tests did not show visible cracks in most specimens tested and failure was considered with change displacement signal using sensitive equipment control.

Stress gradient depends on loading characteristics and the second and third rows of holes of mesh cages show up like critical regions possible for failures. It is suggested modifying the shape of the holes of mesh cages using different diameters and drilling holes to minimize the local stress levels.

Loads used here, in general, are above would occur “in vivo” and indicate that probably the cages tested must support a higher cycle’s number. However, values above were obtained considering pure compression case, and in practice, the spine suffers different loading configurations, which will be evaluated in the next study.

6. ACKNOWLEDGEMENTS

The authors gratefully acknowledge the financial support of the funding agencies (FAPEMIG, CNPq and CAPES) and the support of the FEMEC/UFU, LPM/UFU, and Company Neoortho Orthopedics Products Corporation.

7. REFERENCES

Bellabarba Carlo; Mirza K. Sohail; Chapman R. Jeans. "Biomateriais e suas Aplicações na Cirurgia da Coluna". Cirurgia da Coluna Princípios e Prática. Rio de Janeiro: DiLivros. p 35-65, 2007.

Bernhardt M.; Bridwell, K. H. "Segmental analysis of the sagittal plane alignment of the normal thoracic and lumbar spines and thoracolumbar junction". Spine. 1989;14(7):717-21.

Brantley, A. G.; Maufeild, J. K.; Koeneman, J. B. "The Effects of Pedicle Screw Fit an In Vitro Study". Spine, Philadelphia, v. 1, n. 19, p. 1752-58, Aug. 1994.

Browner, B. D.; Jupiter, J. B.; Levine, A. M.; Trafton, P. G. "Skeletal trauma". 2 ª ed. Philadelphia: Saunders, 1998.

Chen SI, Lin RM, Chang CH. Biomechanical investigation of pedicle screw-ver-tebrae complex: a finite element approach using bonded and contact interface conditions. Med Eng Phys. 2003; 25:275-82.

Ghanayem AJ, Rapiff AJ, Zdeblick TA. "Biomechanical analysis of intervertebral fusion cages with respect to point of insertion and posterior element deficiencies". Presented at International Society for the Study of the Lumbar Spine, Burlington, Vermont, June 25-29, 1996.

Hamill, J; Knutzen, K. M. "Bases biomecânicas do movimento humano". Sâo Paulo: Malone, 1999.

Hao-Che Chuang, Der-Yang Cho, Cheng-Siu Chang, Wen-Yuen Lee, Chen Jung-Chung, Han-Chung Lee, Chun-Chung Chen. "Efficacy and safety of the use of titanium mesh cages and anterior cervical plates for interbody fusion after anterior cervical corpectomy". Surgical Neurology 2006; vol.65: p.464-471.

Hirano T; Hasegawa K; Takahashi HE; Uchiyama, S; Hara T; Washio T; SugiuraT; Yokaichiya M; Ikeda M. "Structural Characteristics of Pedicle and Its Role in screw Stability". Spine, n.22:21, p.2504-10, 1997.

Hirokawa, S.; Yamamoto, k.; kawada, T., 1998, "A photoelastic study of ligament strain". IEEE transactions on rehabilitation engineering, Vol. 6, p. 300-308.

Panjabi, M. M., Kothe, R.; O'Holleran, D.; Liu, W.; Panjabi, M. M. "Internal architecture of the thoracic pedicle: an anatomic study". Spine. 1996. v. 21, n.3, p. 264-70.

Kuhn, A.; Mc Iff, J.; Baumgart, F. W.; Rahn, B. A. "Bone deformation by thread-cutting and thread-forming cortex screws". Injury, v. 26 Supplement 1, p. 12-20, 1995.

Matuoka, C. M.; Basile Júnior, R. "Estudo Anatômico do Pedículo Vertebral Lombar e Estruturas Neurais Adjacentes". Acta Ortopédica Brasileira. 2002. v. 10, n.3, p. 25-34.

Nandan L. Nerurkar, Dawn M. Elliott, Robert L. Mauck. "Mechanical design criteria for intervertebral disk tissue engineering". Journal of Biomechanics 2010; vol.43: p. 1017-1030.

Ray C. D. "Threaded titanium cages for lumbar interbody fusions". Spine 1997; 22:667-79.

Tencer A. F.; Hampton D, Eddy S. "Biomechanical properties of threaded inserts for lumbar interbody spinal fusion". Spine 1995; 20:2408-14.

Yuan H, Kuslich SD, T. Z, Zucherman J. "Two-year follow-up results of an interbody fusion device: open and laparoscopic approaches". Presented at Proceedings of the Tenth Annual European Congress of Neurosurgery, Berlin, Germany, 1995.